ELSEVIER

Journal of Organometallic Chemistry 497 (1995) 119–125

Journal of Organometallic Chemistry

Stereochemical nonrigidity in metallocenium ions ☆

A.R. Siedle *, R.A. Newmark

3M Corporate Research Laboratories, St. Paul, MN 55144, USA

Received 10 January 1995

Abstract

Dynamic NMR spectroscopy of the $MeB(C_6F_5)_3^-$ salts of a series of ring-substituted zirconium- and hafnium-containing metallocenium ions, exemplified by $(RCp)_2ZrCH_3^+$, reveals two exchange processes. One, having the lower free energy of activation, involves shift of the CH_3 group from one lateral equatorial orbital to the other. The second results from exchange between the metal–CH_3 and B–CH_3 groups. Effects of structural variations on exchange barriers are discussed and related to metallocenium ion-catalyzed olefin polymerization.

Keywords: Metallocenium ions; Stereochemical nonrigidity; Zirconium; Hafnium

1. Introduction

Dynamic processes leading to stereochemical nonrigidity have been a classical theme in inorganic and organometallic chemistry [1]. They lead to facile permutation of several atomic (or group) positions. In certain cases, depending on the time scale of the experimental probe, a molecule may appear to have higher symmetry than that of an instantaneous or ''frozen'' structure [2]. Frequently, the barriers to such rearrangements are ca. ≥ 8 kcal mol^{-1} in which case the chemistry may be conveniently studied by NMR. Recently, the extensive reaction chemistry of Group IV metallocenium ions, exemplified by Cp_2ZrMe^+, has been developed. Interest in these organometallic cations has been propelled primarily by recognition of their role in catalytic polymerization of olefins [3]. In this paper, we describe the intramolecular dynamic behavior of a series of metallocenium ions; and also intermolecular (or interion pair) reactions with the associated, weakly coordinating anion. The experimental probe is dynamic NMR (DNMR). Both reactions bear directly on the stereochemical integrity of sites at which olefin polymerization transpires, on solvent effects and on catalyst deactivation.

2. Results and discussion

Reaction of dimethylmetallocenes, exemplified by Cp_2ZrMe_2, with tris(pentafluorophenyl)borane in toluene results in formal transfer of CH_3^- from zirconium to boron (Eq. 1).

$$Cp_2ZrMe_2 + (C_6F_5)_3B \rightarrow [Cp_2ZrMe][MeB(C_6F_5)_3] \qquad (1)$$

and the formation of the $MeB(C_6F_5)_3^-$ salt of the metallocenium ion Cp_2ZrMe^+ [4,5] The solid state structures of several such Zr-containing metallocenium ions have been elucidated by X-ray diffraction and shown to feature $Zr \cdots H_3C{-}B$ interactions the precise details of which require additional study; importantly, the structures do not indicate the presence of an α-agostic Zr–H–C interaction. However, it is the solution state behavior of these metallocenium ions that is of interest here. The 14-electron Cp_2ZrMe^+ ion is extremely Lewis acidic. None of its salts can be dissolved in liquids, e.g. aromatic hydrocarbons, that cannot be viewed as being, at least to some degree, potentially interactive. Thus, there is no prior assurance that the $Zr \cdots H_3C{-}B$ moiety found in the solid persists in solution, although we believe that it does. Weak (at least) interaction of Cp_2ZrMe^+ with toluene, the solvent used in the studies reported here, could well occur. Indeed, Eisch and Pombrik have proposed that Cp_2TiCl^+ forms a π-complex with mesitylene [6]. Even so, the solid state ion pair structures of metallocenium salts provide a heuristi-

---

☆ Dedicated to Professor Hans-H. Brintzinger on the occasion of his 60th birthday.

* Corresponding author.

SSDI 0022-328X(95)00114-X

cally useful framework for visualization of the experimental results and we so employ them here in a simple way.

DNMR spectroscopy reveals that suitably substituted $[(RCp)_2ZrMe]$ $[MeB(C_6F_5)_3]$ salts in toluene display two distinct dynamic processes. The first, which has the lower free energy of activation, is intramolecular (or intracationic) and results in the averaging of the 1,4 and 2,3 positions in the cyclopentadienyl ring which are nonequivalent by symmetry in the solid state. We consider that this reaction, termed methyl shift, involves cleavage of the weakest bond in the salt, the $Zr \cdots H_3C{-}B$ bond, and the formation of a solvent-caged ion pair

$$\begin{aligned}&(RCp)_2ZrMe \cdots H_3C{-}B(C_6F_5)_3\\&\quad\rightarrow [(RCp)_2ZrMe][MeB(C_6F_5)_3] \qquad (2)\end{aligned}$$

This averaging is observable by coalescence of the 1,4 and 2,3 ring ^1H or ^{13}C nuclei or of the nuclei in the ring substituents. In the MO description of Cp_2M^{2+}, there are three vacant metal-centered orbitals in the equatorial plane between the two Cp ligands, two lateral and one central one. (7) In Cp_2ZrMe^+, the methyl group occupies one of these lateral sites. The observed rearrangement in $(RCp)_2ZrMe^+$ can be conceptually accomplished by shift of the CH_3 group from one lateral orbital to the other.

The second dynamic process is intermolecular (or interionic) and involves cleavage of the second weakest bond (vide infra) in the salt, that between boron and CH_3, a reaction that is the microscopic reverse of the synthetic method, Eq. (1). It leads to interchange of the methyl groups bound to boron and to zirconium and is observable as coalescence of the ^1H signals from these two groups. We refer to this as methyl transfer. Fig. 1 displays ^1H NMR spectra of $[(indenyl)_2ZrMe]$ $[MeB(C_6F_5)_3]$ in toluene-d_8. The indenyl ligand is effectively a 1,2-disubstituted (annelated) Cp ligand and, in it, the 1,3 protons are diastereotopic. Fig. 1 shows how, as the temperature is increased, the H(1) and H(3) proton signals at 5.70 and 5.38 ppm coalesce due to methyl shift whilst H(2) at 5.58 ppm remains a sharp triplet; and how, at higher temperature, the $Zr{-}CH_3$ (−0.58 ppm) and $B{-}CH_3$ (−0.23 ppm) signals broaden as a result of intermolecular methyl shift (the −0.23 ppm $B{-}CH_3$ peak is already broad due to interaction with the ^{11}B quadrupole).

There is, admittedly, much about the fine details of these rearrangements that remains to be understood. In particular, one would like to have a more incisive understanding of the solution state structures of metallocenium ions, the nature of interactions with solvents and the details of the intramolecular methyl shift, i.e. whether it is a 1–2 or 1–3 shift and whether α-agostic interactions are involved. But even now, there are compelling reasons to examine what is known about the descriptive chemistry. The degenerate intra- and intermolecular rearrangements are among the simplest possible reactions of metallocenium ions and a better understanding of them is critical to understanding the more complex reactions involved in catalyzed olefin polymerization.

Table 1 presents the free energies of activation for methyl shift and methyl transfer in a series of 0.01–0.05 M zirconium and hafnium metallocenium $MeB(C_6F_5)_3^-$ salts in toluene. Before discussing the effect of structural variations on these barriers, we describe the effect of some experimental variables that shed some light on the dynamic processes.

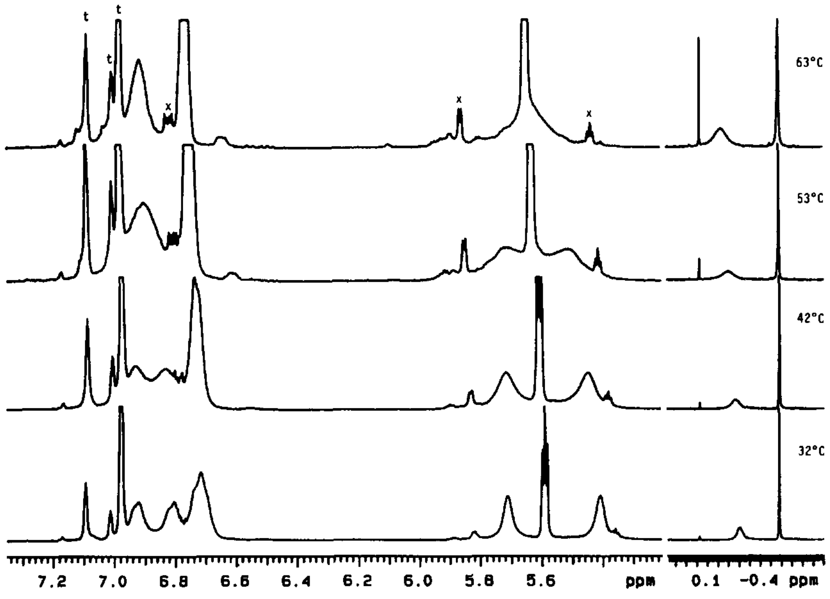

Fig. 1. Variable temperature ^1H NMR spectra of $[(indenyl)_2ZrMe][MeB(C_6F_5)_3]$. t = toluene peaks, x = impuries.

Table 1
Free energies (kcal mol^{-1} ±0.2) for rearrangements in metallocenium $MeB(C_6F_5)_3^-$ salts in toluene

Cation	$\Delta G^{\neq}$, Me shift	$\Delta G^{\neq}$, Me transfer
$(PhCH_2SiMe_2Cp)_2ZrMe^+$	14.7	14.6
$[1,3\text{-}(Me_3Si)_2Cp]_2HfMe^+$	14.3	15.2
$Me_2Si(C_5H_4)_2ZrMe^+$	17.1	17.7
$(Me_3SiCp)_2ZrMe^+$	15.1	> 18.5
$(Me_3SiCp)_2HfMe^+$	15.4	16.5
$(t\text{-}BuCp)_2ZrMe^+$	12.3	17.5
$(Me_3GeCp)_2ZrMe^+$	15.7	18.6
$(Me_3SiCH_2Cp)_2ZrMe^+$	16.6	17.9
$[(9\text{-fluorenyl})CMe_2Cp]ZrMe^+$	> 19	> 19
$[1,2\text{-}(indenyl)_2C_2H_4]ZrMe^+$	–	*rac* 18.4
		meso 18.9
$[1,2\text{-}(indenyl)_2C_2H_4]HfMe^+$	–	*rac* 16.5
		meso 18.1
$[1,2\text{-}(H_4indenyl)_2C_2H_4]ZrMe^+$	–	*meso* 18.4
$(indenyl)_2ZrMe^+$	15.8	18.1
$(indenyl)_2HfMe^+$	15.4	16.2
$(fluorenyl)_2ZrMe^+$	13.5	> 19
$[1,2\text{-}(9\text{-fluorenyl})_2C_2H_4]ZrMe^+$	17.5	17.7
$[1,2\text{-}(9\text{-fluorenyl})_2C_2H_4]HfMe^+$	14.7	14.6
$[(9\text{-fluorenyl})_2SiMe_2]ZrMe^+$	17.0	16.8

The effect of temperature on barriers to methyl shift and transfer is smaller than the experimental uncertainties, ±0.2 kcal mol^{-1}, and so the entropies of activation for these reactions are small or zero. This indicates that, for methyl shift, the cation and anion do not separate and move far apart; and suggests that the transition state may resemble a solvent separated or encaged ion pair. For $[(indenyl)_2ZrMe][MeB(C_6F_5)_3]$, the barrier to methyl shift is unchanged as the concentration is varied five fold, providing further evidence for an intramolecular (intracationic) process. We observe no effect on the rate of methyl shift upon adding additional $(C_6F_3)_3B$. However, addition of extra $(indenyl)_2ZrMe_2$ increases the rate of methyl exchange (observed as line broadening), possibly through a methyl-bridged species such as $(indenyl)_2Zr(CH_3)\text{–}(CH_3)\text{–}Zr(CH_3)(indenyl)_2^+$ [8]. In toluene solution, when *rac*- and *meso*-$[1,2\text{-}(indenyl)_2C_2H_4ZrMe][MeB(C_6F_5)_3]$ (M = Zr, Hf), are mixed together, they show separate ^1H and ^{11}B signals for the $B\text{–}CH_3$ portion of the anion, cf. Table 2. The isomeric *rac*- and *meso*-metallocenium ions independently participate in the methyl shift reaction and remain associated with their respective $MeB(C_6F_5)_3^-$ anions, which do not interconvert, up to at least 50°C. This result strongly suggests that methyl shift involves the metallocenium salt in a solvent cage and implies that much of the solid-state cation–anion interaction illuminated by X-ray crystallography persists in hydrocarbon solvents. Using $[(indenyl)_2Zr(CD_3)][CD_3B(C_6F_5)_3]$, we sought evidence for a kinetic deuterium isotope effect. However, the changes in indenyl proton lifetimes caused by H/D substitution were less than the experimental errors involved in their determination. One can only conclude that shift of the $Zr\text{–}CH_3$ group does not involve significant Zr–H(D) interaction in the transition state.

The barrier to methyl shift in $(indenyl)_2ZrMe^+$, 15.8 kcal mol^{-1} in toluene, is substantially reduced in solvents of higher dielectric constant. In both dichloromethane and chlorobenzene, $\Delta G^{\neq}$ drops to 8.0 kcal mol^{-1}; but the entropy of activation decreases to −19 e.u. The barrier to methyl transfer is, in contrast, unchanged within experimental error. We interpret these effects as indicative of stabilization of the solvent separated ion pair by the solvent dipoles. The large negative entropy of activation implies orientation of these dipoles and/or weak interaction of the metallocenium ion with the chlorine-containing solvents. Organometallic complexes of halocarbons are now well known (9). The metallocenium ion–solvent interaction is, however, probably quite weak and, in the limit when a metallocenium ion is complexed to a strong σ-donor such as a tertiary phosphine, the resulting complex is stereochemically rigid, possibly as a result of β-agostic interactions and/or tight binding of the 2e donor [3]. Use of halogenated solvents can, therefore, produce kinetic effects not directly associated with increased dielectric constant but the experimental results are discordant. Enhancement of rates of propylene polymerization catalyzed by metallocenium $MeB(C_6F_5)_3^-$ salts on going from toluene to *o*-dichlorobenzene has been reported but solvent effects were quite small when methylaluminoxane was used to generate the metallocenium ion [10,11]. Other workers have observed an accelerative effect of dichloromethane in methylaluminoxane-containing catalyst systems [12].

We argue that the barrier to methyl shift contains two terms. The first is disruption of the interaction between the metallocenium ion and the associated anion. The second term is an intrinsic barrier, such as might be observed in the gas phase or in the absence of strong interactions with solvent or other species present in solution. Methyl shift is unobservable in $[1,2\text{-}(9\text{-fluorenyl})_2C_2H_4]ZrMe^+$ generated from $(MeAlO)_x$ and $[(fluorenyl)_2C_2H_4]ZrX_2$ (X = Cl, CH_3) because it forms a complex with trimethylaluminum, a quotidian impurity in the aluminoxane. This complex presumably contains the $Zr(\mu\text{-}Me_2)AlMe_2$ moiety identified by Bochman [8] and its formation is revealed by the 30 nm bathochromic shift in the cation LMCT band. Even so, the aluminoxane-derived complex exhibits higher olefin polymerization rates that the simple $MeB(C_6F_5)_3^-$ derivative [10,13,14].

Bulky substituents on the cyclopentadienyl rings should promote cation–anion separation for steric reasons and such substituents tend to lower barriers to intramolecular methyl shift. For example, they are 15.4 kcal mol^{-1} for $(Me_3SiCp)_2HfMe^+$ and 14.3 kcal mol^{-1} for $[1,3\text{-}(Me_3Si)_2Cp]_2HfMe^+$, cf. Table 1.

Table 2
NME data for metallocenium $MeB(C_6F_5)_3^-$ salts [a]

$(PhCH_2SiMe_2Cp)_2ZrMe^+$ ^{1}H: 7.13 (t, 7, Ph), 7.06 (t, 7, Ph), 6.59 (d, 7, Ph), 6.03, 5.96, 5.85 5.77 (Cp), 1.82 (CH_2), 0.20 ($ZrCH_3$) ^{13}C: 125.3 (C *ipso*), 124.4, 121.6, 117.5, 42.3 ($ZrCH_3$) 27.2 (CH_2), 22.2 (BCH_3) −3.3 ($SiCH_3$). ^{29}Si: −4.8.

$[(Me_3Si)_2Cp]_2HfMe^+$ ^{1}H: 6.75 (H2), 6.24, 5.89 (H4,5), 0.72 (BCH_3), 0.46 ($HfCH_3$), 0.06 ($SiCH_3$). ^{13}C: 135.9 (C2), 122.7 (C4,5), 41.7 ($HfCH_3$), −0.41 ($SiCH_3$). ^{29}Si: −5.4.

$Me_2Si(C_5H_4)_2ZrMe^+$ ^{1}H: 6.39, 6.27, 5.37, 4.96 (Cp), 0.6 (BCH_3), 0.36 ($ZrCH_3$), 0.08, −0.08 ($SiCH_3$). ^{13}C: 125.5, 122.3, 118.5, 112.1 (Cp), 41.5 ($ZrCH_3$). ^{29}Si: −13.5.

$(Me_3SiCp)_2ZrMe^+$ ^{1}H: 6.22, 6.02, 5.85 (Cp), 0.50 (ZrMe, J_{CH} 122), 0.35 (BCH_3), −0.03 ($SiCH_3$). ^{13}C: 125.5 (C *ipso*), 124.5, 121.5, 117.8, 117.2 (Cp), 41.9 ($ZrCH_3$), 23.9 (BCH_3), −0.7 ($SiCH_3$). ^{29}Si: −5.6.

$(Me_3SiCp)_2HfMe^+$ ^{1}H: 6.21, 5.97, 5.79 (Cp), 0.57 (BCH_3), 0.27 ($HfCH_3$), −0.01 ($SiCH_3$). ^{13}C: 123.98, 123.9 (C *ipso*), 121.1, 116.3, 115.8 (Cp), 40.7 ($HfCH_3$), 22.0 (BCH_3), −0.6 ($SiCH_3$). ^{29}Si: −5.6.

$(t\text{-}BuCp)_2ZrMe^+$ [b] ^{1}H: 5.85, 5.83, 5.58, 5.38 (Cp), 0.79 (t-Bu), 0.63 ($ZrCH_3$), 0.37 (BCH_3) ^{13}C: 115.0, 114.7 (Cp *ipso*), 113.3, 113.0, 112.3 (Cp), 43.0 ($ZrCH_3$), 33.3 (t-Bu quat. C), 30.9 (t-Bu CH_3), 21 (BCH_3).

$(Me_3GeCp)_2ZrMe^+$ ^{1}H: 6.21, 6.00, 5.97, 5.86 (Cp), 0.48 ($ZrCH_3$), 0.23 (BCH_3), 0.11 ($GeCH_3$). ^{13}C: 127.1 (C *ipso*), 123.9, 121.1, 117.0, 116.5 (Cp), 41.3 ($ZrCH_3$), 24 (BCH_3), −1.0 ($GeCH_3$).

$[(fluorenyl)\text{-}CMe_2\text{-}Cp]ZrMe^+$ ^{1}H: 7.64, 7.60, 7.02, 6.93 (d, 8, of m, flu), 7.13, 6.74, 6.63, 6.41 (t, 8, of m, flu), 5.94, 5.54, 5.20, 4.47 (q, *J* = 2, Cp), 1.52, 1.47 (CCH_3), −0.53 (BCH_3), −0.92 ($ZrCH_3$). ^{13}C: 130.0, 129.3, 128.3, 126.5, 126.3, 124.6, 124.5 (Flu), 118.9, 112.9, 106.0, 101.5 (Cp), 43.2 ($ZrCH_3$), 40.4 (Me_2C), 27.9, 27.7 (CCH_3), 23 (BCH_3).

$[rac\text{-}(indenyl)_2C_2H_4]ZrMe^+$ ^{1}H: 5.96 (AB quartet), 2.65, 2.55 (CH_2), 0.4 (BCH_3), −1.85 ($ZrCH_3$). ^{11}B: −13.5. ^{13}C: 52.4 ($ZrCH_3$), 27.4 (CH_2).

$[meso\text{-}(indenyl)_2C_2H_4]ZrMe^+$ ^{1}H: 6.33, 5.23 (AX mult), 5.88, 5.67 (AX mult) 2.81, 2.68 (CH_2), −0.46 ($ZrCH_3$), −0.65 (BCH_3). ^{11}B: −13.1.
^{13}C: 116.2, 114.9, 112.6, 104.4, 104.0, 47.6 ($ZrCH_3$), 28.6 (CH_2).

$[rac\text{-}(indenyl)_2C_2H_4]HfMe^+$ ^{1}H: 0.67 (BCH_3), −2.10 ($HfCH_3$). ^{11}B: −12.4. ^{13}C: 44.5 ($HfCH_3$), 26.7 (CH_2).

$[meso\text{-}(indenyl)_2C_2H_4]HfMe^+$ ^{1}H: 6.23, 5.07 (AX mult), 5.94, 5.78 (AX mult), −0.40 (BCH_3), −0.70 ($HfCH_3$). ^{11}B: −12.7. ^{13}C: 114.5, 114.3, 111.0, 108.6, 101.8, 101.7, 46.9 ($HfCH_3$), 27.9 (CH_2).

$[meso\text{-}(H_4indenyl)_2C_2H_4]ZrMe^+$ ^{1}H: 6.07, 5.55, 5.29, 4.64 (2 3 Hz AX doublets), 2.7–0.7 (multiplets, CH_2), 0.55 ($HfCH_3$), 0.2 (BCH_3). ^{13}C: 133.1, 132.6, 131.6, 130.9, 126.6, 124.3 (Cp quaternary C), 118.3, 112.3, 111.9, 107.4 (sp^2 CH), 43.9 ($ZrCH_3$), 28.3, 27.6, 24.2, 24.1, 23.7, 23.6, 22.3, 22.1, 21.9 (CH_2).

$(indenyl)_2ZrMe^+$ ^{1}H: 6.91, 6.80, 6.73, 6.68 (H4–7), 5.70, 5.38 (H1,3), 5.58 (t, 3, H2), −0.3 (BCH_3), −0.58 ($ZrCH_3$). ^{13}C: 129.3, 128.2, 126.2, 125.6, 119.2 (C2), 103.5, 102.6, 47.9 ($ZrCH_3$), 19 (BCH_3).

$(indenyl)_2HfMe^+$ ^{1}H: 6.92, 6.84 (H6,7), 6.74, 6.68 (H5,8), 5.53, 5.30 (H1,3), 5.59 (H2), 0.04 (BCH_3), −0.72 ($HfCH_3$). ^{13}C: 119.2(C2), 101.4, 100.4 (C1,3), 45.4 (J_{CH} 120, $HfCH_3$), 17.8 (BCH_3).

$(fluorenyl)_2ZrMe^+$ [c] ^{1}H: 7.34 (d, 8, H4), 7.07 (d, 8, H5), 7.02 (t, 8, H3), 6.90 (t, 8, H2), 6.81 (d, 8, H1), 6.75 (d, 8, H8), 6.54 (t, H7), 6.52 (t, H6), 5.15 (s, H9), −0.37 ($ZrCH_3$), −0.7 (BCH_3).

$[1,2\text{-}(9\text{-}fluorenyl)_2C_2H_4]ZrMe^+$ [c] ^{1}H: 7.66 (d, 8, H5), 7.25 (d, 9, H4), 7.08 (d, 9, H1), 7.02 (t, 8, H6), 6.87 (d, 9, H8), 6.71 (2H, t, 8, H2, 7), 6.09 (t, 8, H3), 3.63, 3.42 (AA′BB′, CH_2), −1.43 (BCH_3), −1.48 ($ZrCH_3$).

$[1,2\text{-}(9\text{-}fluorenyl)_2C_2H_4]HfMe^+$ ^{1}H: 7.66 (d, 8, H5), 7.25 (d, 9, H4), 7.08 (d, 9, H1), 7.02 (t, 8, H6), 6.87 (d, 9, H8), 6.71 (2H, t, 8, H2, 7), 6.09 (t, 8, H3), 3.74, 3.53 (br m), −1.2 (BCH_3), −1.78 ($HfCH_3$).

$[(9\text{-}fluorenyl)_2SiMe_2]ZrMe^+$ ^{1}H: 7.82 (d, 8, H1), 6.66 (t, 8, H2), 6.63 (t, 8, H7), 6.07 (H3), −0.60 ($SiCH_3$), −1.5 (BCH_3), −1.54 ($ZrCH_3$).

[a] In toluene at 25°C unless otherwise noted. [b] At −42°C. [c] ^{1}H assignments obtained from COSY and TOCSY spectra.

Metallocenium ions in which the carbocyclic ligands are connected by a one-atom bridge, i.e. $Me_2Si(C_5H_4)_2ZrMe^+$, $[(9\text{-fluorenyl})\text{–}CMe_2\text{–}Cp]ZrMe^+$ and $[Me_2Si(9\text{-fluorenyl})_2]ZrMe^+$, have relatively higher barriers to methyl shift as indicated in Table 1. We suggest two reasons for this effect. First, the steric effect of the bridge is to open the ring centroid–Zr–ring centroid angle, also seen in related thorium compounds [15], making the metal more accessible to the anion. Second, the steric effect leads to reduced carbon–metal orbital overlap, making the metal more electron deficient, reflected in Zr core level binding energies [16], and strengthening cation–anion interactions. For one or both reasons, contributions of the cation–anion separation terms to the net barriers are anticipated.

There appear to be no clear trends for the role of the metal atom in the intramolecular rearrangement. Barriers are comparable for the $(Me_3SiCp)_2MMe^+$ and $(indenyl)_2MMe^+$ pairs for M = zirconium and hafnium but higher for zirconium relative to hafnium in $[1,2\text{-}(9\text{-fluorenyl})_2C_2H_4]MMe^+$. The compound $[(indenyl)_2TiMe][MeB(C_6F_5)_3]$ had insufficient solubility in toluene for DNMR experiments.

For the intermolecular methyl transfer process, the data indicate that bulky ring substituents increase free energies of activation to methyl exchange between the metal atom and boron. Introduction of one- or two-atom bridges between the carbocyclic rings produces no clear trends. However, in the three pairs of metallocenium ions just mentioned, it is evident that barriers to methyl shift are 2–3 kcal mol^{-1} lower for hafnium than zirconium. These trends can be simply rationalized in terms of the higher metal–carbon bond disruption energies for hafnium than zirconium [17].

2.1. Relationship to olefin polymerization chemistry

The effect of varying solvents on dynamic processes in metallocenium ions and polymerization activity has been mentioned above. There are several situations where these rearrangements seem directly relevant. The compound *rac*-[*anti*-$Me_4Cp\text{-}C_2H_4$-(indenyl)]$TiCl_2$, when treated with methylaluminoxane, affords a catalyst that produces a crystalline–amorphous block polypropylene. It has been proposed that the metallocenium ion active site may exist in two isomeric states and that there is frequent isomerization between the two during growth of a single polymer chain [18–20]. It was concluded that the atactic segments contained 50–100 monomer units and that there were 20–50 units long depending on reaction temperature; and further that the catalytic species was fluxional (or isomerized) with a rate constant of 0.2–2 s. at 25–50 °C. From these data, one can calculate that the free energy barrier for movement of the polymer chain between the two nonequivalent sites is about 18 kcal mol^{-1}, which is consistent with the barriers to methyl shift in Table 1.

In careful studies of propylene polymerization catalyzed by [(9-fluorenyl)–CMe_2–Cp]$ZrCl_2$ and $(MeAlO)_x$, *m* diads in the syndiotactic polymer were observed. The concentration of these *m* defects decreased asymptotically with propylene concentration. Several explanations have been put forth. One is that a "skipped insertion" results from isomerization of the coordinatively unsaturated metallocenium intermediate, i.e. [(9-fluorenyl)–CMe_2–Cp]Zr–$(C_3H_6)_nR^+$ (R = CH_3 or H). Another involves collapse of a species in which two molecules of propylene are coordinated to the above intermediate and in which the growing polymer chain occupies the central position at zirconium [21,22]. We prefer the latter on the ground that the barrier we observe in [(9-fluorenyl)–CMe_2–Cp]$ZrMe^+$ (> 19 kcal mol^{-1}; the sample decomposed before the fast exchange limit could be reached) seems too large to account for a "skipped insertion" process. Possibly, a further reduction could result from agostic interactions between zirconium and hydrogen atoms in the polymer chain. However, there is no firm experimental evidence for such interactions or that agostic interactions would be favored over coordination to propylene or solvent [23]. To clarify this point, it would be desirable to study the dynamic properties of metallocenium ions containing longer alkyl groups in place of methyl.

We have depicted the interionic exchange of methyl groups bound to zirconium and to boron as cleavage of the B–CH_3 bond as though it were the weakest bond in the $MeB(C_6F_5)_3^-$ anion. It is not always the weakest and if, instead, the B–C_6F_5 bond were cleaved, then transfer of a C_6F_5 group to zirconium would result.

$$[(RCp)_2ZrMe][MeB(C_6F_5)_3] \rightarrow (RCp)_2Zr(Me)(C_6F_5) + MeB(C_6F_5)_2 \qquad (3)$$

Table 3
NMR data for some dimethylmethylmetallocenes [a]

$(PhCH_2SiMe_2Cp)_2ZrMe_2$	^{1}H: 7.10 (H_p), 6.98 (H_m), 6.83 (H_o), 5.93, 5.89 (Cp), 2.40 (CH_2), 0.12 ($SiCH_3$), −0.27 ($ZrCH_3$). ^{13}C: 139.8 (C_{ipso}), 128.7 (C_o), 128.5 (C_m), 124.5 (C_p), 118.2, 113.6 (Cp), 29.9 ($ZrCH_3$), 27.8 (CH_2), −2.5 ($SiCH_3$).
$[1,3-(Me_3Si)_2Cp]_2HfMe_2$	^{1}H: 6.85 (H1), 5.94 (d, 2, H4,5), 0.27 ($SiCH_3$), −0.25 ($HfCH_3$). ^{13}C: 133.4 (C2), 122.7 (C1,3), 115.7 (C4,5), 36.8 ($HfCH_3$), 0.44 ($SiCH_3$).
$(Me_3SiCH_2Cp)_2ZrMe_2$	^{1}H: 5.61 (H2,5), 5.52 (H3,4), 1.89 (CH_2), 0.05 ($SiCH_3$), −0.13 ($ZrCH_3$). ^{13}C: 126.0 (C1), 110.4 (C2,5), 107.1 (C3,4), 30.5 ($ZrCH_3$), 20.9 (CH_2), −1.76 ($SiCH_3$. ^{29}Si: 1.7.
$(t-BuCp)_2ZrMe_2$	^{1}H: 5.80, 5.75 (Cp), 1.12 (CCH_3), −0.08 ($ZrCH_3$). ^{13}C: 138.9 (C1), 109.8, 108.3 (Cp), 33.0 (*C*CH_3), 31.9 (C*C*H_3), 31.4 ($ZrCH_3$).
$(Me_3GeCp)_2ZrMe_2$	^{1}H: 6.02 (d, 2, H2,5), 5.89 (d, 2, H3,4), 0.30 ($GeCH_3$), −0.20 ($ZrCH_3$). ^{13}C: 120.6 (C1), 117.3 (C2,5), 113.5 (C3,4), 30.3 ($ZrCH_3$), 0.3 ($GeCH_3$).
$(indenyl)_2HfMe_2$	^{1}H: 7.18, 6.88 (AA′XX′), 5.68 (d, 3, H1,3), 5.56 (t, 3 H2), −1.00 ($HfCH_3$).
$(fluorenyl)_2ZrMe_2$	^{1}H: 7.64 (H1), 7.03 (H2), 6.99 (H4), 6.96 (H3), 5.41 (H9), −1.74 ($ZrCH_3$).
$[1,2-(9-fluorenyl)_2C_2H_4]ZrMe_2$ [b]	^{1}H: 7.79 (d, 8), 7.60 (d, 8), 7.18 (t, 8), 7.07 (t,8), 4.03 (CH_2), −2.46 ($ZrCH_3$). ^{13}C: 127.5 (C_{ipso}), 126.4, 124.6, 122.4, 122.0 (ring CH), 118.1 (C_{ipso}), 98.9 (C9), 41.1 ($ZrCH_3$), 27.9 (CH_2).
$[1,2-(9-fluorenyl)_2C_2H_4]HfMe_2$ [b]	^{1}H: 7.81 (d, 8), 7.71 (d, 8), 7.20 (t, 8), 7.06 (t, 8), 4.13 (CH_2), −2.71 ($HfCH_3$). ^{13}C: 127.4 (C_{ipso}), 126.2, 124.6, 122.2, 122.0 (ring CH), 117.7 (C_{ipso}), 98.5 (C9), 27.2 ($HfCH_3$).
$[(9-fluorenyl)_2SiMe_2]ZrMe_2$ [b]	^{1}H: 7.89 (dd, 8, 1, H4,5), 7.68 (dd, 8, 1, H1,8), 7.27 (ddd, 8, 7, 1, H3,6), 7.00 (ddd, 8, 7, 1, H2,7), 1.44 ($SiCH_3$), −2.54 ($ZrCH_3$). ^{13}C: 131.4 (C4a,5a), 126.7 (C2,7), 125.6 (C1,8), 124.5 (C1a,8a), 124.1 (C4,5), 123.3 (C3,6), 62.3 (C9), 41.4 ($ZrCH_3$), 3.2 ($SiCH_3$).

[a] In toluene-d_8. [b] In CD_2Cl_2.

When $(fluorenyl)_2ZrMe_2$ was treated with $(C_6F_5)_3B \cdot C_{18}H_{37}OH$ to generate $(fluorenyl)_2ZrMe^+$ [24], extensive ligand redistribution upon standing occurred as indicated by new ^{11}B NMR signals at 86.3, 80.5 and 72.0 ppm. These are assigned to Me_3B, $Me_2B(C_6F_5)$ and $MeB(C_6F_5)_2$ respectively, the latter two because they are close to the arithmetic averages of the ^{11}B chemical shifts of Me_3B (80 ppm) and $(C_6F_5)_3B$ (60 ppm). Interestingly, the amounts of these three-coordinate boron compounds increased when a small amount of 1-hexene was added. Others have also found evidence for methyl-fluoroaryl exchange [4a,25]. Reactions of $(RCp)_2Zr(C_6F_5)^+$ with 1-olefins has not been reported. In the probable event that reactivity is low, replacement of a methyl group or polymer chain by a C_6F_5 would constitute a new catalyst deactivation process.

3. Conclusions

Metallocenium ions of the type $[(RCp)_2MMe]X$ (M = Zr, Hf; X = $MeB(C_6F_5)_3^-$ or $(Me_2AlO)(MeAlO)_{1-x}^-$) are stereochemically nonrigid. Barriers for intramolecular methyl shift in the $MeB(C_6F_5)_3^-$ salts range from 13.5 to > 19 kcal mol^{-1}. Barriers to intermolecular transfer of methyl groups between M and $MeB(C_6F_5)$ are higher and range from 14.6 to > 19 kcal mol^{-1}. To the extent that a methyl group may serve as a model for a growing polymer chain, isomerization that shifts the chain from one lateral site to the other is a process having a substantial free energy of activation.

4. Experimental

Tris(pentafluorophenyl)boron was obtained by the method of Massey and Park and purified by vacuum sublimation [26]. Metallocenium $MeB(C_6F_5)_3^-$ salts were prepared in resealable NMR tubes under nitrogen ($[O_2] < 2$ ppm) by the combination in toluene-d_8 (vacuum transferred from NaK) of the dimethylmetallocene with a stoichiometric amount of $(C_6F_3)_3B$. Their ^1H, ^{13}C and ^{29}Si NMR chemical shifts, obtained on a Varian XL-400 spectrometer at 25 °C (i.e. in the slow exchange limit) are collected in Table 2 and expressed relative to internal Me_4Si. ^{11}B chemical shifts are referenced to external $BF_3 \cdot OEt_2$. Dynamic NMR spectra were analyzed following procedures described previously. Lifetimes for the methyl shift exchange process were calculated from the linewidths of ligand ring protons using the equations of Gutowsky and Holm [27]. Lifetimes for protons involved in the methyl shift reaction were calculated from the linewidth of the MCH_3 (M = Zr or Hf) resonances. In all cases, the linewidths were corrected for linewidth in the absence of exchange, taken as the linewidth of a sharp solvent resonance in the sample [28].

New dimethylmetallocenes, whose ^1H and ^{13}C NMR chemical shifts are collected in Table 3, were prepared by methylation of the corresponding metallocene dichlorides with methyllithium in diethyl ether at 0–10 °C. The metallocene dichlorides were synthesized by the reaction of the Li^+ salts of the appropriate ligands with $ZrCl_4$ in dichloromethane at −78 °C using standard methods [29]. The compounds $Me_2Si(C_5H_4)_2ZrMe_2$ [16], [(fluorenyl)-CMe_2-Cp]$ZrMe_2$ [22], [(indenyl)$_2C_2H_4$]MMe_2 [23], [(H_4indenyl)$_2C_2H_4$]$ZrMe_2$ [30], (indenyl)$_2MMe_2$ [31], (fluorenyl)$_2ZrMe_2$ [32], [(fluorenyl)$_2C_2H_4$]MCl_2 [33] and [Me_2Si(fluorenyl)$_2$]$ZrCl_2$ [33] were prepared by literature methods.

4.1. $(PhCH_2SiMe_2Cp)_2ZrCl_2$

A solution of $K[C_5H_5]$ in 100 ml 1,2-dimethoxyethane, prepared from 2.3 g (35 mmol) C_5H_6 and KH, was added dropwise to 6.5 g $PhCH_2SiMe_2Cl$ (Petrarch) in 30 ml of the same solvent. After stirring overnight, 14 ml of a 2.5 M solution of butyl-lithium in hexane was added followed, after 0.5 h, by 4.0 g (17 mmol) $ZrCl_4$ dissolved in 40 ml dimethoxyethane. After stirring 16 h, the solvents were evaporated and the residue extracted with 150 ml boiling heptane. Concentration and cooling of the extract provided 4.5 g product as white needles. Anal.: Calc. (Found) for $C_{28}H_{34}Cl_2Si_2Zr$ C, 57.1 (56.8); H, 5.8 (5.8). NMR ($CDCl_3$): ^1H: 7.16 (H_m), 7.06 (H_p), 6.87 (H_o), 6.53 (H2,5), 5.45 (H3,4), 2.26 (CH_2), 0.28 (CH_3).

4.2. $[(Me_3Si)_2Cp]_2HfCl_2$

Butyllithium, 27 ml of a 2 M solution in hexane, was added to 7.5 g (54 mmol) $Me_3SiC_5H_5$ (Aldrich) in 150 ml toluene at −78 °C. When the reaction mixture had warmed to 0 °C 5.88 g (54 mmol) Me_3SiCl in 20 ml toluene was added dropwise with stirring. After 16 h, it was recooled to −78 °C and 27 ml 2M butyllithium in hexane added. At 25 °C, 8.6 g (27 mmol) solid $HfCl_4$ was added. After refluxing and vigorous stirring for 16 h, the reaction mixture was filtered hot through Celite and the solvents evaporated. Two recrystallizations of the residue from heptane afforded 3.1 g product. Anal.: Calc. (Found) for $C_{22}H_{42}Cl_2HfSi_4$ C, 39.6 (39.3); H, 6.3 (6.1). NMR ($CDCl_3$): ^1H: 6.89 (H_2), 6.34 (H4,5), 0.28 (CH_3). ^{13}C: 141.7 (C2), 126.7 (C1,3), 119.1 (C4,5), 0.06 ($SiCH_3$). ^{29}Si: 6.0.

4.3. $[(Me_3Si)_2Cp]_2HfMe_2$

A solution of 1.0 g (1.5 mmol) $[(Me_3Si)_2Cp]_2HfCl_2$ in 10 ml diethyl ether was treated at −78°C with 2.0 ml 1.5 M CH_3Li in ether. The cold bath was removed and the reaction mixture stirred for 1 hr at 25 °C. Ether was removed on the vacuum line. Vacuum sublimation of the residue afforded 0.5 g product as a white solid.

4.4. $(t\text{-}BuCp)_2ZrMe_2$

Methyllithium, 34 ml of a 1.4 M solution in diethyl ether, was added to 5 g (47 mmol) dimethylfulvene in 50 ml ether. Next, a solution of 6.1 g $ZrCl_4$ in 85 ml 1,2-dimethoxyethane was added dropwise with stirring. After 16 h, the reaction mixture was filtered through Celite and the solvents evaporated. The residue was extracted with 200 ml boiling heptane. Concentration and cooling of the extract produced 6 g product as white needles which were further purified by vacuum sublimation. Anal.: Calc. (Found) for $C_{18}H_{26}Cl_2Zr$ C, 53.5 (53.5); H, 6.4 (6.4). NMR ($CDCl_3$): ^1H: 6.42 (H3), 6.30 (H2), 1.32 (CH_3). ^{13}C: 144.1 (C1), 115.5 (C2), 112.2 (C3), 33.4 (C–CH_3), 31.1 (CH_3).

A solution of 2.02 g (5 mmol) $(t\text{-}BuCp)_2ZrCl_2$ in 40 ml diethyl ether was cooled to −78 °C and an ether solution containing 10 mmol CH_3Li added. The reaction mixture was warmed to room temperature, stirred for 1 h after which the solvent was evaporated. Two recrystallizations of the residue from hexane at −78 °C afforded 1.1 g white, microcrystalline product.

References and notes

[1] L.M. Jackman and F.A. Cotton (Eds.) *Dynamic Nuclear Magnetic Resonance Spectroscopy*, Academic Press, 1975.

[2] E.L. Muetterties, *Inorg. Chem.*, *4* (1965) 769.

[3] R.F. Jordan, *Adv. Organomet. Chem.*, *32* (1991) 325.

[4] (a) X. Yang, C.L. Stern and T.J. Marks, *J. Am. Chem. Soc.*, *116* (1994) 10015; (b) X. Yang, C.L. Stern and T.J. Marks, *J. Am. Chem. Soc.*, *113* (1991) 3623; (c) P.A. Deck and T.J. Marks, Abstracts of Papers, *207th ACS Meeting, INOR-45* (1994).

[5] J.A. Ewen and M.J. Elder, *Can. Pat. Appl.*, 2,027,145.

[6] J.J. Eisch, S.I. Pombrik and G.-X. Zheng, *Macromol. Chem. Macromol. Symp.*, *66* (1993) 109.

[7] J.W. Lauher and R.W. Hoffmann, *J. Am. Chem. Soc.*, *98* (1976) 1729.

[8] (a) M. Bochman, S.J. Lancaster, M.B. Hursthouse and K.M.A. Malik, *Organometallics*, *13* (1994) 2235; (b) M. Bochman and S.J. Lancaster, *Angew. Chem. Int. Ed.*, *33* (1994) 1634.

[9] R.J. Kulawiec and R.H. Crabtree, *Coord. Chem. Rev.*, *99* (1990) 89.

[10] J.C.W. Chien, W. Song and M.D. Rausch, *J. Polym. Sci.*, *32A* (1994) 2387.

[11] J.C. Vizzini, J.C.W. Chien, G.N. Babu and R.A. Newmark, *J. Polym. Sci.*, *32A* (1994) 2049.

[12] N. Herfert and G. Fink, *Makromol. Chem.*, *193* (1992) 773.

[13] A.R. Siedle, B. Hanggi, R.A. Newmark, K. Mann and M. Ryan, *Macromol. Chem. Macromol. Symp.*, *89* (1995) 299.

[14] Other examples of counterion effects have been reported: X. Yang, C.L. Stern and T.J. Marks, *Organometallics*, *10* (1991) 840.

[15] C.M. Fendrick, L.D. Schertz, V.W. Day and T.J. Marks, *Organometallics*, *7* (1988) 1828.

[16] A.R. Siedle, R.A. Newmark, W.M. Lamanna and J.N. Schroepfer, *Polyhedron*, *9* (1990) 301.

[17] L.E. Schock and T.J. Marks, *J. Am. Chem. Soc.*, *110* (1988) 7701.

[18] G.H. Llinas, S.-H. Dong, D.T. Malin, M.D. Rausch, Y.-G. Lin, H.H. Winter and J.C.W. Chien, *Macromolecules*, *25* (1992) 1242.

[19] J.C.W. Chien, G.H. Llinas, M.D. Rausch, Y.-G. Lin, H.H. Winter, J.L. Atwood and S.G. Bott, *J. Polym. Sci.*, *30A* (1992) 2601.

[20] D.T. Malin, M.D. Rausch, Y.-G. Lin, S.H. Dong and J.C.W. Chien, *J. Am. Chem. Soc.*, *112* (1990) 2030.

[21] J.A. Ewen, M.J. Elder, R.L. Jones, S. Curtis and H.N. Cheng, in T. Keii and K. Soga (Eds.), *Cataytic Olefin Polymerization*, Elsevier, 1990, p. 439.

[22] J.A. Ewen, M.J. Elder, R.L. Jones, L. Haspeslagh, J.L. Atwood, S.G. Bott and K. Robinson, *Makromol. Chem. Macromol. Symp.*, *48/49* (1991) 253.

[23] In the compound $(\eta^3\text{-}C_7H_7)Mo(CO)_2[B(pyrazolyl)_2Et_2]$, an Mo–C–H agostic involving the B-ethyl group prevails over a η^5 structure having no agostic interaction cf. M. Brookhart, M.L.H. Green and L.-L. Wong, *Prog. Inorg. Chem.*, *36* (1988) 4.

[24] A.R. Siedle and W.M. Lamanna, U.S. Pat., 5,296,433 (3/22/94).

[25] A.D. Horton and A.G. Orpen, *Organometallics*, *10* (1991) 3910.

[26] A.G. Massey and A.J. Park, *J. Organomet. Chem.*, *5* (1966) 218.

[27] H.S. Gutowsky and C.H. Holm, *J. Chem. Phys.*, *25* (1956) 1228.

[28] R.A. Newmark, *J. Chem. Ed.*, *60* (1983) 45.

[29] W. Spaleck, F. Kuber, A. Winter, J. Rohrmann, B. Bachmann, M. Antberg, V. Dolle and E.I. Paulus, *Organometallics*, *13* (1994) 954.

[30] R.B. Grossman, R.A. Doyle and S.L. Buchwald, *Organometallics*, *10* (1991) 1501.

[31] E. Samuel and M.D. Rausch, *J. Am. Chem. Soc.*, *95* (1973) 6263.

[32] E. Samuel, H.G. Alt, D.C. Hrncir and M.D. Rausch, *J. Organomet. Chem.*, *113* (1976) 331.

[33] H.G. Alt, W. Milius and S.J. Palackal, *J. Organomet. Chem.*, *472* (1994) 113.